Process for Growth of Group-IV Alloys Containing Tin by Remote Plasma Enhanced Chemical Vapor Deposition

Bruce Claflin[1*], G J. Grzybowski[2], A M. Kiefer[1], M E. Ware[3], S Zollner[4]

[1]Air Force Research Laboratory, United States, [2]KBR, United States, [3]University of Arkansas, United States, [4]New Mexico State University, United States

Submitted to Journal:
Frontiers in Materials

Specialty Section:
Translational Materials Science

Article type:
Original Research Article

Manuscript ID:
521063

Received on:
17 Dec 2019

Frontiers website link:
www.frontiersin.org

Conflict of interest statement

The authors declare that the research was conducted in the absence of any commercial or financial relationships that could be construed as a potential conflict of interest

Author contribution statement

BC, GJG, and AMK contributed conception and design of the study; BC, GJG, MEW, and SZ provided analysis and interpretation of data for the work; BC wrote the first draft of the manuscript; GJG, SZ, MEW, and BC made substantial contributions to acquisition, analysis and interpretation of data for the work. All authors contributed to manuscript revision, read and approved the submitted version.

Keywords

RPECVD, characterization, Growth process, GeSn and GeSiSn alloys, Crystalline

Abstract

Word count: 131

A remote plasma enhanced chemical vapor deposition process using GeH_4, SiH_4 and $SnCl_4$ precursors has been developed for epitaxial growth of group-IV alloys directly on Si (001) substrates, without the need for buffer layers. X-ray diffraction measurements of a representative $Ge_{1-x}Sn_x$ sample which is 233 nm thick, with x = 9.6% show it to be highly oriented along the [001] direction and nearly relaxed, with 0.37% compressive strain. Ellipsometry measurements provide a pseudo-dielectric function which is well fitted by a 3-layer (substrate/alloy/surface oxide) model. Cross-sectional transmission-electron-microscope images show a highly defective interface layer, ~ 60 nm thick, containing edge dislocations and stacking faults; above this layer, the lattice is well-ordered, with a much lower density of defects. Atomic force microscopy measurements show an RMS roughness of 1.2 nm for this film.

Contribution to the field

Alloying tin with germanium and silicon produces materials that can efficiently absorb infra-red light and be integrated with electronic control circuitry. However, the solubility of tin in germanium and silicon is very low making synthesis of these alloys challenging and requiring the development of specialized deposition processes. A remote plasma enhanced chemical vapor deposition (RPECVD) process using germane, silane, and tin chloride precursors has been developed for growth of nearly strain relaxed, group-IV alloys containing tin, directly on silicon substrates, without the need for buffer layers. Single crystal alloy films with up to 10% tin incorporation have been demonstrated without surface segregation of tin. This remote plasma process uses energy transfer from plasma-excited He to activate the chemical precursors, thereby removing the need for their thermal activation on the substrate surface. This decoupling of the substrate temperature from precursor decomposition allows for independent control of the growth temperature to optimize desired film characteristics. In addition, RPECVD provides a simple process for group-IV alloy growth on silicon since buffer layers are not required to produce good structural quality. Finally, the RPECVD process uses a precursor partial pressure ratio that is commensurate with the target film composition, resulting in a much more efficient use of these precursors.

Ethics statements

Studies involving animal subjects

Generated Statement: No animal studies are presented in this manuscript.

Studies involving human subjects

Generated Statement: No human studies are presented in this manuscript.

Inclusion of identifiable human data

Generated Statement: No potentially identifiable human images or data is presented in this study.

Data availability statement

Generated Statement: The datasets generated for this study are available on request to the corresponding author.

Process for Growth of Group-IV Alloys Containing Tin by Remote Plasma Enhanced Chemical Vapor Deposition

B. Claflin[1], G. J. Grzybowski[2], M. E. Ware[3], S. Zollner[4], and A. M. Kiefer[1]

[1] Air Force Research Laboratory, Sensors Directorate, Wright-Patterson Air Force Base,
OH 45433

[2] KBR, 2601 Mission Point Blvd., Suite 300, Dayton, OH 45431

[3] University of Arkansas, Fayetteville, AR, 72701

[4] New Mexico State University, Las Cruces, NM, 88003

ABSTRACT

A remote plasma enhanced chemical vapor deposition process using GeH_4, SiH_4 and $SnCl_4$ precursors has been developed for epitaxial growth of group-IV alloys directly on Si (001) substrates, without the need for buffer layers. X-ray diffraction measurements of a representative $Ge_{1-x}Sn_x$ sample which is 233 nm thick, with x = 9.6% show it to be highly oriented along the [001] direction and nearly relaxed, with 0.37% compressive strain. Ellipsometry measurements provide a pseudo-dielectric function which is well fitted by a 3-layer (substrate/alloy/surface oxide) model. Cross-sectional transmission-electron-microscope images show a highly defective interface layer, ~ 60 nm thick, containing edge dislocations and stacking faults; above this layer, the lattice is well-ordered, with a much lower density of defects. Atomic force microscopy measurements show an RMS roughness of 1.2 nm for this film.

INTRODUCTION

Semiconductor devices based on the group-IV elements Si and Ge, as well as their alloys, have dominated many applications in the electronics industry, such as microprocessors for logic circuits, cell phones, global positioning systems (GPS) and wireless communications (WiFi). However, similar progress in optical and electro-optical devices has been limited by the indirect nature of the fundamental energy gap in these materials. In contrast, cubic α-Sn is a zero bandgap, group-IV semiconductor which, when combined in sufficient concentration with Ge, results in a $Ge_{1-x}Sn_x$ alloy with a direct bandgap [1-6]. These $Ge_{1-x}Sn_x$ alloys have attracted attention as potential low-cost detectors [7-9] and emitters [10-12] in the short- and mid-wave-infrared (SWIR and MWIR) spectral regions and can be incorporated into a variety of components [13-15] for Si-based integrated photonics. Further alloying $Ge_{1-x}Sn_x$ with Si produces a ternary alloy, $Ge_{1-x-y}Si_ySn_x$, which allows independent control of lattice constant and bandgap energy [16, 17].

One significant challenge in the synthesis of Sn-containing group-IV alloys is that the solubility of Sn is ~ 1% in Ge [18] and ~ 0.1% in Si [19]. As a result of these limitations, low temperature, non-equilibrium growth methods are required to deposit $Ge_{1-x}Sn_x$ and $Ge_{1-x-y}Si_ySn_x$ alloys. Early attempts to produce $Ge_{1-x}Sn_x$ films by sputtering [20-22] or molecular beam epitaxy [23-31] showed limited success, with growth on different substrates (Ge, GaAs) to minimize the lattice mismatch. Many of these samples were amorphous or the crystalline quality was not very high, and film growth was susceptible to Sn segregation.

A major advance in Sn-containing group-IV alloy synthesis was the development of a chemical vapor deposition (CVD) process [32-34] using SnD_4 as the Sn precursor. High quality samples were prepared and characterized, and photoluminescence (PL) was demonstrated for the first time [35, 36]. Higher order germanes and silanes have subsequently been used to increase the reactivity of the precursors, allowing growth at lower temperatures [37-39]. However, the lack of a commercial supplier for SnD_4 and its limited thermal stability led to the identification of $SnCl_4$, a liquid with a reasonably high vapor pressure, as an alternative [40] CVD Sn precursor.

Reduced pressure CVD using $SnCl_4$ has become the preferred method of $Ge_{1-x}Sn_x$ growth and has attracted interest in these alloys. High quality $Ge_{1-x}Sn_x$ films with Sn concentrations as high as $x = 0.3$ have been reported [41-45] and optically pumped lasers have been demonstrated [46-52] at temperatures up to 273 K. Still, this reduced pressure CVD process requires a very high precursor partial pressure ratio [53], $P_{Ge_2H_6}/P_{SnCl_4} > 100$, to achieve substitutional Sn incorporation with a high degree of crystallinity. In addition, this approach typically requires growth of one or more buffer layers (Ge and/or $Ge_{1-x}Sn_x$), sometimes referred to as a virtual substrate, especially for samples with the highest Sn content.

A variation of this method of growth, remote plasma enhanced chemical vapor deposition (RPECVD) [54], has been used previously to synthesize Si [55, 56], Ge [57], and $Si_{1-x}Ge_x$ [58, 59] films at lower temperatures than those used in conventional CVD processes. In the RPECVD process, an inert gas, typically He or Ar, is excited using an inductively coupled plasma source, and the plasma excited species subsequently interacts with precursor gases introduced downstream, activating them for growth on the substrate. This alternative process for precursor activation allows for thin-film deposition of group-IV alloys at reduced substrate temperatures.

This work describes a process for synthesizing Sn-containing group-IV alloys, directly on Si substrates, using RPECVD to activate GeH_4, SiH_4 and $SnCl_4$ precursors. The physical, structural, and optical characteristics of a representative $Ge_{1-x}Sn_x$ sample grown using this RPECVD process are also presented.

EXPERIMENT

Epitaxy of group-IV alloys containing Sn, grown directly on 2-inch Si substrates, without buffer layers, has been performed via an RPECVD process in a custom designed, ultra-high-vacuum (UHV) chamber using a top-mounted Advanced Energy Litmas RPS 3001 inductively coupled remote plasma tube, as shown schematically in Fig. 1. Equipment details for this RPECVD reactor will be published separately [60]. Growths of Sn-containing group-IV alloy films have been demonstrated over a range of substrate temperatures, from 295 - 340 °C as measured by a thermocouple, and chamber pressures, from 200 – 800 mTorr. The Si substrates receive a dilute (2.5%) $HF:H_2O$ dip to remove their native surface oxide prior to loading into the growth chamber and are heated to the deposition temperature in flowing He prior to flowing precursor gases and initiating the remote plasma.

For a representative $Ge_{1-x}Sn_x$ film growth on a 2-inch, p-type, Si (100) substrate, a flow of He gas at 50 SCCM was injected upstream of the RF coil and excited with 1 kW of plasma power. A 50 SCCM flow of 2% GeH_4 diluted in He was introduced through a gas dispersal ring, downstream from the plasma as shown in Fig. 1. Similarly, a 12.5 SCCM flow of He carrier gas was used to entrain liquid $SnCl_4$ vapor through a bubbler, resulting in a ~ 2% concentration which was injected through a separate gas injector ring, downstream of the He plasma. A substrate temperature of 325 ℃ and a chamber pressure of 535 mTorr were maintained throughout this film growth.

Film thickness and uniformity of this $Ge_{1-x}Sn_x$ sample were measured by optical interference with a Filmetrics F50 Thin Film Mapper tool. The pseudo-dielectric function of the film was determined at a 70º angle of incidence from 0.6 - 4.7 eV in 0.01 eV steps using a Jobin Yvon Horiba UVISEL phase modulated spectroscopic ellipsometer. The data were fitted in a three-layer (substrate/alloy/oxide) model using the WVASE32 software of the J. A. Woolam Company. The optical constants of the alloy were described using a parametric semiconductor model [6]. Reciprocal space maps (RSM) of the $(\bar{2}\bar{2}4)$ reflection and $2\theta-\omega$ scans of the (004) reflection were performed using a PANanalyical Empyrean X-ray diffractometer. Film composition and strain were determined [61, 62] using these measured values of lattice parameters and the elastic constants for Ge and Sn. Cross-sectional, bright field, transmission-electron-microscopy (TEM) along the <110> direction was used to evaluate the crystalline structure of the layer as well as to investigate the substrate/film interface. Finally, surface roughness of the sample was measured using a Bruker Dimension atomic force microscope (AFM) in tapping-mode.

RESULTS AND DISCUSSION

The RPECVD process provides a robust and reproducible method to synthesize group-IV alloys containing Sn over a range of compositions: $Ge_{1-x}Sn_x$ films have been produced with Sn concentrations as high as 10%, without surface Sn segregation, as well as $Ge_{1-x-y}Si_ySn_x$ and $Si_{1-x}Sn_x$ layers. The relative incorporation of each constituent generally reflects the gas flow ratios of the corresponding precursors. Furthermore, RPECVD provides considerable flexibility in process development to optimize specific material properties of interest.

A representative example using this RPECVD process is a $Ge_{1-x}Sn_x$ sample with a thickness of 233 nm, grown at a rate of 2.2 nm/min. Thickness uniformity is typically better than 10% across a 2 inch wafer as a result of the flow dynamics of the reactor, even without the use of sample rotation. It should be noted that without plasma excitation, there is no film deposition under the growth conditions used. Ellipsometry data were well fitted with a 3-layer model (substrate/alloy/surface oxide), as shown in Fig. 2, giving an alloy thickness of 217 nm and a surface oxide thickness of 3.9 nm. The oscillations below 2 eV in the pseudo-dielectric function are the result of interference fringes from the film.

An X-ray $2\theta-\omega$ scan along [001] superimposed on a corresponding $(\bar{2}\bar{2}4)$ RSM for the representative $Ge_{1-x}Sn_x$ sample are shown in Fig. 3. A (004) $Ge_{1-x}Sn_x$ peak at $2\theta = 64.85º$ is observed and the RSM shows an asymmetrical $(\bar{2}\bar{2}4)$ reflection that lies close to the relaxation line, indicating that the film is nearly strain relaxed. From the measured lattice constant values, a 9.6% Sn content and 0.37% compressive strain are inferred for this sample. Quantitative values of Sn content derived from X-ray measurements for $Ge_{1-x}Sn_x$ films grown by RPECVD have been confirmed by Rutherford backscattering (RBS) measurements (not shown) on a number of separate samples.

A cross-sectional TEM image of the representative $Ge_{1-x}Sn_x$ alloy is shown in Fig. 4. An interface layer which is ~ 60 nm thick contains a high density of edge dislocations and stacking faults, and possible strain fields extending into the substrate. Above this interface layer, the crystalline quality of the film improves dramatically and the defect density decreases so that individual threading dislocations can be imaged. The defective interface layer accommodates much of the strain due to the lattice mismatch of $Ge_{1-x}Sn_x$ and Si, allowing the bulk of the film to relax, consistent with the X-ray results. Most of the edge dislocations and stacking faults within this ~ 60 nm layer appear to annihilate, resulting in improved crystallinity and a lower defect density above it.

Figure 5 shows a 10 µm x 10 µm AFM image of the sample surface. The film is quite smooth, with an RMS roughness of 1.2 nm. There is no indication of the crosshatching which is typically seen in the growth of thick Ge films on Si as a result of strain relaxation from misfit dislocation formation and motion along the Ge/Si interface. This lack of structure on the surface indicates that a different strain relief mechanism dominates in RPECVD alloy films, consistent with the TEM results.

CONCLUSIONS

An RPECVD process using GeH_4, SiH_4 and $SnCl_4$ precursors has been developed for growth of nearly strain relaxed, group-IV alloys containing Sn, directly on Si substrates, without the need for buffer layers. Single crystal alloy films with up to 10% Sn incorporation have been demonstrated without surface segregation of Sn. This remote plasma process uses energy transfer from plasma-excited He to activate the chemical precursors, thereby removing the need for their thermal activation on the substrate surface. This decoupling of the substrate temperature from precursor decomposition allows for independent control of the growth temperature to optimize desired film characteristics. In addition, RPECVD provides a simple process for group-IV alloy growth on Si since buffer layers are not required to produce good structural quality. Finally, the RPECVD process uses a precursor partial pressure ratio that is commensurate with the target film composition, resulting in a much more efficient use of these precursors.

A representative $Ge_{1-x}Sn_x$ sample synthesized using this RPECVD process has x = 9.6% Sn incorporation and is nearly strain relaxed. Cross-sectional TEM shows a highly defective interface layer ~ 60 nm thick resulting in a nearly strain relaxed film. The sample surface is very smooth, with an RMS roughness of 1.2 nm as measured by AFM.

ACKNOWLEDGMENTS

The authors would like to thank Malak Refaei for preparation of the TEM samples and Mourad Benamara for performing the TEM measurements. This work was supported by AFOSR LRIR 16RYCOR333 and 19RYCOR032 (G. Pomrenke)

REFERENCES

[1] S. Zaima, O. Nakatsuka, N. Taoka, M. Kurosawa, W. Takeuchi, and M. Sakashita, Sci. Technol. Adv. Mater. **16**, 043502 (2015).

[2] J. Mathews, R. T. Beeler, J. Tolle, C. Xu, R. Roucka, J. Kouvetakis, and J. Menéndez, Appl. Phys. Lett. **97**, 221912 (2010).

[3] P. Moontragoon, R. A. Soref, Z. Ikonic, J. Appl. Phys. **112**, 073106 (2012).

[4] A. A. Tonkikh, C. Eisenschmidt, V. G. Talalaev, N. D. Zakharov, J.Schilling, G. Schmidt, P. Werner, Appl. Phys. Lett. **103**, 032106 (2013).

[5] S. Gupta, B. Magyari-Köpe, Y. Nishi, and K. C. Saraswat, J. Appl. Phys. **113**, 073707 (2013).

[6] N. S. Fernando, R. A. Carrasco, R. Hickey, J. Hart, R. Hazbun, S. Schoeche, J. N. Hilfiker, J. Kolodzey S. Zollner, J. Vac. Sci. Technol. B **36**, 021202 (2018).

[7] C. Chang, H. Li, C.-T. Ku, S.-G. Yang, H. H. Cheng, J. Hendrickson, R. A. Soref, and G. Sun, Appl. Opt. **55**, 10170 (2016).

[8] H. S. Maczko, R. Kudrawiec & M. Gladysiewicz, Sci. Rep. **6**, 34082 (2016).

[9] C-H. Tsai, G-E. Chang, Proc. SPIE **10231**, Optical Sensors 2017, 102310J (2017).

[10] S. Wirths, R. Geiger, N. Von Den Driesch, G. Mussler, T. Stoica, S. Mantl, Z. Ikonic, M. Luysberg, S. Shiussi, J. H. Hartmann, H. Sigg, J. Faist, D. Buca, and D. Grutzmacher, Nat. Photon. **9**, 88 (2015).

[11] Y. Zhou, W. Dou, W. Du, T. Pham, S. A. Ghetmiri, S. Al-Kabi, A. Mosleh, M. Alher, J. Margetis, J. Tolle, G. Sun, R. Soref, B. Li, M. Mortzazvi, H. Naseem, and S-Q. Yu, J. Appl. Phys., **120**, 023102 (2016).

[12] J. Margetis, S. Al-Kabi, W. Du, W. Dou, Y. Zhou, T. Pham, P. Grant, S. Ghetmiri, A. Mosleh, B. Li, J. Liu, G. Sun, R. Soref, J. Tolle, M. Mortzazvi, S-Q. Yu, ACS Photonics **5**, 827 (2018).

[13] R. Soref, Phil. Trans. R. Soc. A **372**, 20130113 (2014).

[14] G. Sun, H. H. Cheng, J. Menéndez, J. B. Khurgin, R. A. Soref, Appl. Phys. Lett. **90**, 251105 (2007).

[15] S. Wirths, D. Buca, S. Mantl, Prog. Cryst. Prog. Cryst. Growth Charact. **62**, 1 (2016).

[16] J. Kouvetakis, J. Menendez, and A. G. V. Chizmeshya, Annual Review of Materials Research **36**, 497 (2006).

[17] J. Kouvetakis, V.R. D'Costa, Y.-Y. Fang, J. Tolle, A.V.G. Chizmeshya, J. Xie and J. Menéndez, The Japan Society for Promotion of Science 5th International Symposium, "Advanced science and technology of silicon materials", 352-356 (2008).

[18] R. W. Olesinski and G. J. Abbaschian, Bull. Alloy Phase Diagrams **5**, 265 (1984).

[19] R. W. Olesinski and G. J. Abbaschian, Bull. Alloy Phase Diagrams **5**, 274 (1984).

[20] S. Shah, J.E. Greene, L.L. Abels, Q. Yao, P.M. Raccah, J. Cryst. Growth **83**, 3 (1987),

[21] K. Ishida, H. Myoren, M. Yamamoto, T. Imura, Y. Osaka, Jap. J. Appl. Phys. **28**, L125 (1989).

[22] T. Maruyama, J. Electrochem. Soc. **145**, 1303 (1998).

[23] M.T. Asom, E.A. Fitzgerald, A.R. Kortan, B. Spear, L.C. Kimerling, Appl. Phys. Lett. **55**, 578 (1989).

[24] P.R. Pukite, A. Harwit, S.S. Iyer, Appl. Phys. Lett. **54**, 2142 (1989).

[25] H. Höchst, M.A. Engelhardt, I. Hernandez-Calderon, Phys. Rev. B **40**, 9703 (1989).

[26] J. Piao, J. Vac. Sci. Technol. B **8**, 221 (1990).

[27] E.A. Fitzgerald, P.E. Freeland, M.T. Asom, W.P. Lowe, R.A. Macharrie, B.E. Weir, A. R. Kortan, F. A. Thiel, Y.-H. Xie, A. M. Sergent, S. L. Cooper, G. A. Thomas and L. C. Kimerling, J. Electron. Mater. **20**, 489 (1991).

[28] M. Rojas-López, H. Navarro-Contreras, P. Desjardins, O. Gurdal, N. Taylor, J.R.A. Carlsson, and J. E. Greene, J. Appl. Phys. **84**, 2219 (1998).
[29] K.A. Bratland, Y.L. Foo, T. Spila, H.-S. Seo, R.T. Haasch, P. Desjardins, and J. E. Greene, J. Appl. Phys. **97**, 044904 (2005).
[30] E. Kasper, J. Werner, M. Oehme, S. Escoubas, N. Burle, J. Schulze, Thin Solid Films **520**, 3195 (2012).
[31] M. Oehme, D. Buca, K. Kostecki, S. Wirths, B. Holländer, E. Kasper, J. Schulze, J. Cryst. Growth **384**, 71 (2013).
[32] J. Taraci, S. Zollner, M. R. McCartney, J. Menendez, M. A. Santana-Aranda, D. J. Smith, A. Haaland, A. V. Tutukin, G. Gundersen, G. Wolf, and J. Kouvetakis, J. Am. Chem. Soc. **123**, 10980 (2001).
[33] M. Bauer, J. Taraci, J. Tolle, A. V. G. Chizmeshya, S. Zollner, D. J. Smith, J. Menendez, C. Hu, and J. Kouvetakis, Appl. Phys. Lett. **81**, 2992 (2002).
[34] M. Bauer, C. Ritter, P. A. Crozier, J. Ren, J. Menendez, G. Wolf, and J. Kouvetakis, Appl. Phys. Lett. **83**, 2163 (2003).
[35] R. A. Soref, J. Kouvetakis, J. Menéndez, J. Tolle, and V. R. D'Costa, J. Mater. Res. **22**, 3281 (2007).
[36] J. Mathews, R. T. Beeler, J. Tolle, C. Xu, R. Roucka, J. Kouvetakis, and J. Menéndez, Appl. Phys. Lett. **97**, 221912 (2010).
[37] G. Grzybowski, R. T. Beeler, L. Jiang, D. J. Smith, J. Kouvetakis, J. Menéndez, Applied Physical Letters **101**, 072105, (2012)
[38] G. Grzybowski, L. Jiang, R. T. Beeler, T. Watkins, A. V. G. Chizmeshya, C. Xu, J. Menéndez, J. Kouvetakis, Chemistry of Materials **24**, 1619-1628, (2012)
[39] R. T. Beeler, C. Xu, D. J. Smith, G. Grzybowski, J. Menéndez, J. Kouvetakis, Appl. Phys. Lett **101**, 221111 (2012)
[40] B. Vincent, F. Gencarelli, H. Bender, C. Merckling, B. Douhard, D.H. Petersen, O. Hansen, H. H. Henrichsen, J. Meersschaut, W. Vandervorst, M. Heyns, R. Loo, and M. Caymax, Appl. Phys. Lett. **99**, 152103 (2011).
[41] S. Wirths, D. Buca, Z. Ikonic, P. Harrison, A.T. Tiedemann, B. Holländer, T. Stoica, G. Mussler, U. Breuer, J.M. Hartmann, D. Grützmacher S. Mantl, Thin Solid Films **557**, 183 (2014).
[42] J. Aubin, J.M. Hartmann, J. Cryst. Growth **482**, 30 (2018).
[43] J. Zheng, Z. Liu, Y. Zhang, Y. Zuo, C. Li, C. Xue, B. Cheng, Q. Wang, J. Cryst. Growth **492**, 29 (2018).
[44] D. Imbrenda, R. Hickey, R. A. Carrasco, N. S. Fernando, J. VanDerslice, S. Zollner, and J. Kolodzey, Appl. Phys. Lett. **113**, 122104 (2018).
[45] C. Xu, P. M. Wallace, D. A. Ringwala, S. L. Y. Chang, C. D. Poweleit, J. Kouvetakis, and J. Menendez, Appl. Phys. Lett. **114**, 122104 (2019).
[46] S. Wirths, R. Geiger, N. von den Driesch, G. Mussler, T. Stoica, S. Mantl, Z. Ikonic, M. Luysberg, S. Chiussi, J. M. Hartmann, H. Sigg, J. Faist, D. Buca, and D. Grutzmacher, Nat. Photonics **9**, 88 (2015).

[47] S. Al-Kabi, S. A. Ghetmiri, J. Margetis, T. Pham, Y. Zhou, W. Dou, B. Collier, R. Quinde, W. Du, A. Mosleh, J. Liu, G. Sun, R. A. Soref, J. Tolle, B. Li, M. Mortazavi, H. A. Naseem, and S.-Q. Yu, Appl. Phys. Lett. **109**, 171105 (2016).
[48] D. Stange, S. Wirths, R. Geiger, C. Schulte-Braucks, B. Marzban, N. von den Driesch, G. Mussler, T. Zabel, T. Stoica, J. M. Hartmann, S. Mantl, Z. Ikonic, D. Grutzmacher, H. Sigg, J. Witzens, and D. Buca, ACS Photonics **3**, 1279 (2016).
[49] V. Reboud, A. Gassenq, N. Pauc, J. Aubin, L. Milord, Q. M. Thai, M. Bertrand, K. Guilloy, D. Rouchon, J. Rothman, T. Zabel, F. Armand Pilon, H. Sigg, A. Chelnokov, J. M. Hartmann, and V. Calvo, Appl. Phys. Lett. 111, 092101 (2017).
[50] J. Margetis, S. Al-Kabi, W. Du, W. Dou, Z. Yiyin, T. Pham, P. Grant, S. A. Ghetmiri, M. Aboozar, B. Li, J. Liu, G. Sun, R. A. Soref, J. Tolle, M. Mortazavi, and S.-Q. Yu, ACS Photonics **5**, 827 (2018).
[51] J. Chrétien, N. Pauc, F. A. Pilon, M. Bertrand, Q.-M. Thai, L. Casiez, N. Bernier, H. Dansas, P. Gergaud, E. Delamadeleine, R. Khazaka, H. Sigg, J. Faist, A. Chelnokov, V. Reboud, J.-M. Hartmann, and V. Calvo, ACS Photonics, 6, 10, 2462 (2019).
[52] Y. Zhou, W. Dou, W. Du, S. Ojo, H. Tran, S. Ghetmiri, J. Liu, G. Sun, R. Soref, J. Margetis, J. Tolle, B. Li, Z. Chen, M. Mortazavi, and S. Yu, Conference on Lasers and Electro-Optics, OSA Technical Digest, AW3P.3 (2019).
[53] S. Wirths, D. Buca, S. Mantl, Prog. Cryst. Growth Charact. Mater. **62**, 1 (2016).
[54] L. Bàrdoš, Vacuum **38**, 637 (1988).
[55] R. A. Rudder, G. G. Fountain, and R. J. Markunas, J. Appl. Phys. **60**, 3519 (1986).
[56] G. Lucovsky, P. D. Richard, D. V. Tsu, S. Y. Un, and R. J. Markunas, J. Vac. Sci. Technol. A **4**, 681 (1986).
[57] M. Heintze, C. E. Nebel, and G. H. Bauer, Mat. Res. Soc. Symp. Proc. **192**, 565 (1990).
[58] D. Kinosky, R. Qian, J. Irby, T. Hsu, B. Anthony, S. Banerjee, A. Tasch, C. Magee, C. L. Grove, Appl. Phys. Lett. **59**, 817 (1991).
[59] R. Qian, D. Kinosky, T. Hsu, J, Irby, A. Mahajan, S. Thomas, B. Anthony, S. Banerjee, A. Tasch, L. Rabenberg, C. Magee, J. Vac. Sci. Technol. A **10**, 1920 (1992).
[60] G. J. Grzybowski, A. M. Kiefer, and B. Claflin, manuscript in preparation.
[61] H. J. McSkimin, J. Appl. Phys. **24**, 988 (1953).
[62] C. Xu, C. L. Senaratne, R. J. Culbertson, J. Kouvetakis, and J. Menéndez, J. Appl. Phys. **122**, 125702 (2017).

FIGURE CAPTIONS

Figure 1 Equipment configuration of RPECVD growth chamber

Figure 2 Pseudo-dielectric function of a representative $Ge_{1-x}Sn_x$ film with x= 9.6% Sn incorporation measured by UV spectroscopic ellipsometry. The solid line shows a 3-layer model fit (substrate/alloy/surface oxide).

Figure 3 X-ray diffraction 2θ−ω scan along (004) and RSM map around ($\bar{2}\bar{2}4$) reflection of a representative $Ge_{1-x}Sn_x$ film grown directly on Si.

Figure 4 Cross-sectional, bright field, TEM image taken along the <110> direction of a representative $Ge_{1-x}Sn_x$ film shows a ~ 60 nm thick interface layer with a high density of misfit dislocations and stacking faults. Above this layer, the crystalline quality improves dramatically and the defect density is greatly reduced.

Figure 5 10 μm x 10 μm AFM image of a representative $Ge_{1-x}Sn_x$ film shows a smooth surface (1.2 nm RMS roughness). The cross-hatch pattern typically seen for Ge films grown on Si is not observed.

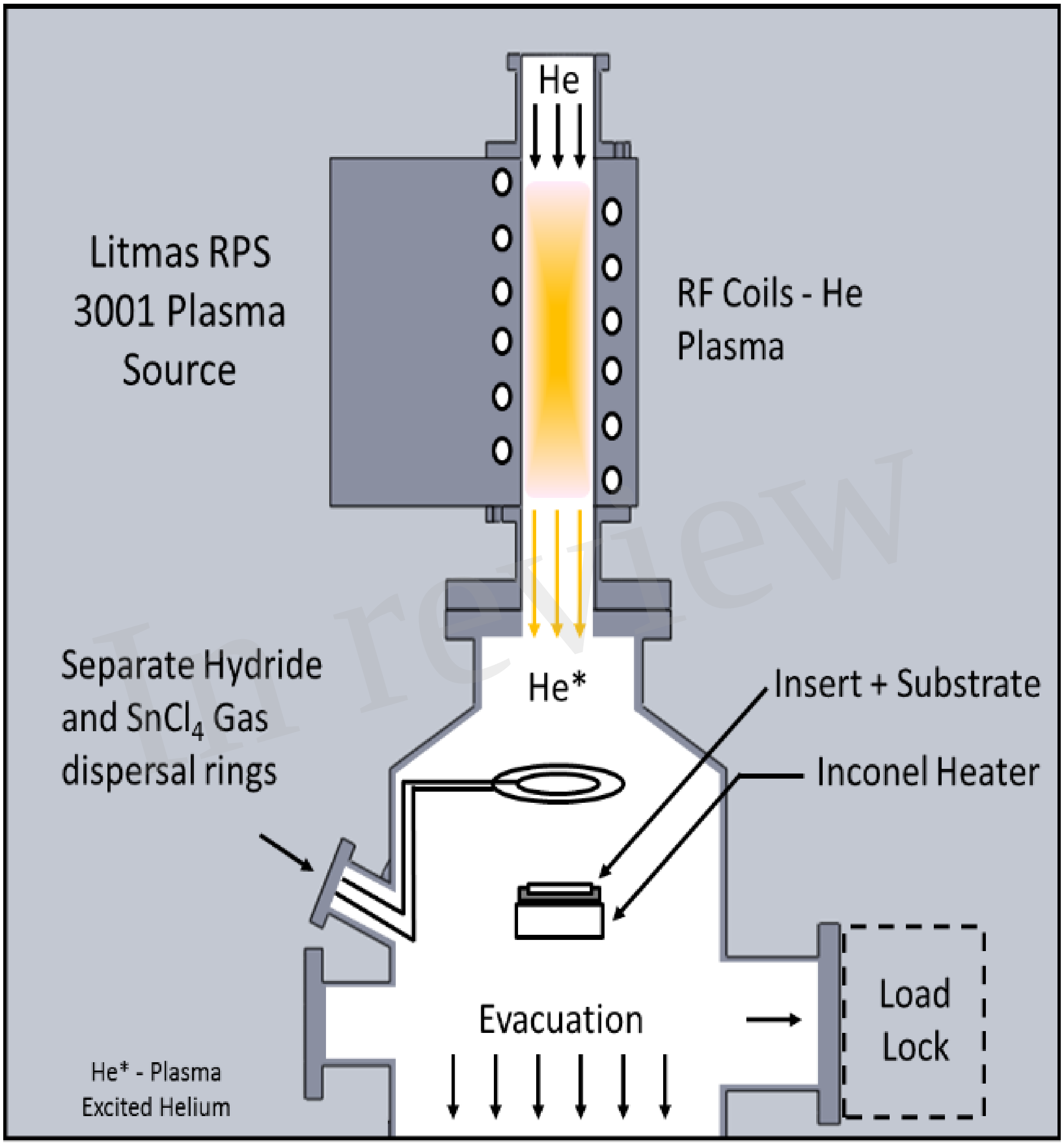
He
Litmas RPS 3001 Plasma Source
RF Coils - He Plasma
He*
Separate Hydride and $SnCl_4$ Gas dispersal rings
Insert + Substrate
Inconel Heater
Evacuation
Load Lock
He* - Plasma Excited Helium

Figure 1

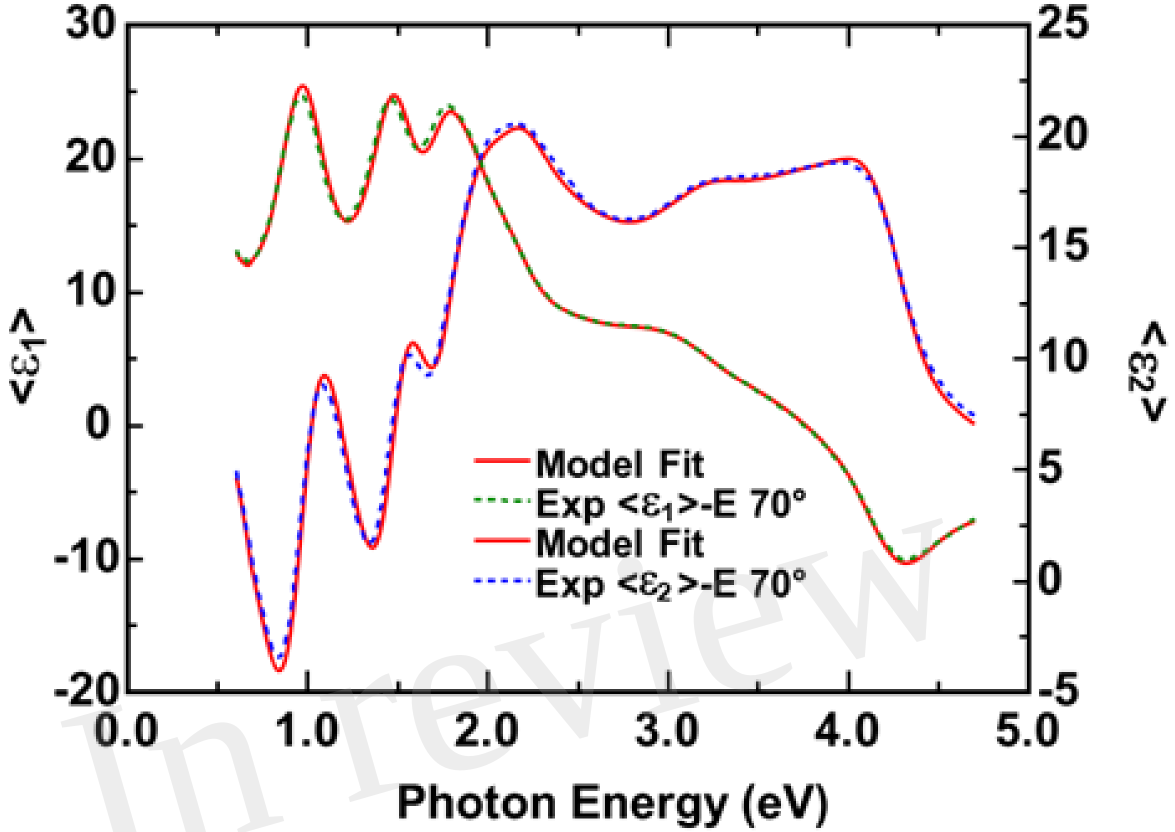
30
20
10
0
-10
-20
<ε1>
25
20
15
10
5
0
-5
<ε2>
0.0
1.0
2.0
3.0
4.0
5.0
Photon Energy (eV)
Model Fit
Exp <ε1>-E 70°
Model Fit
Exp <ε2>-E 70°

Figure 2

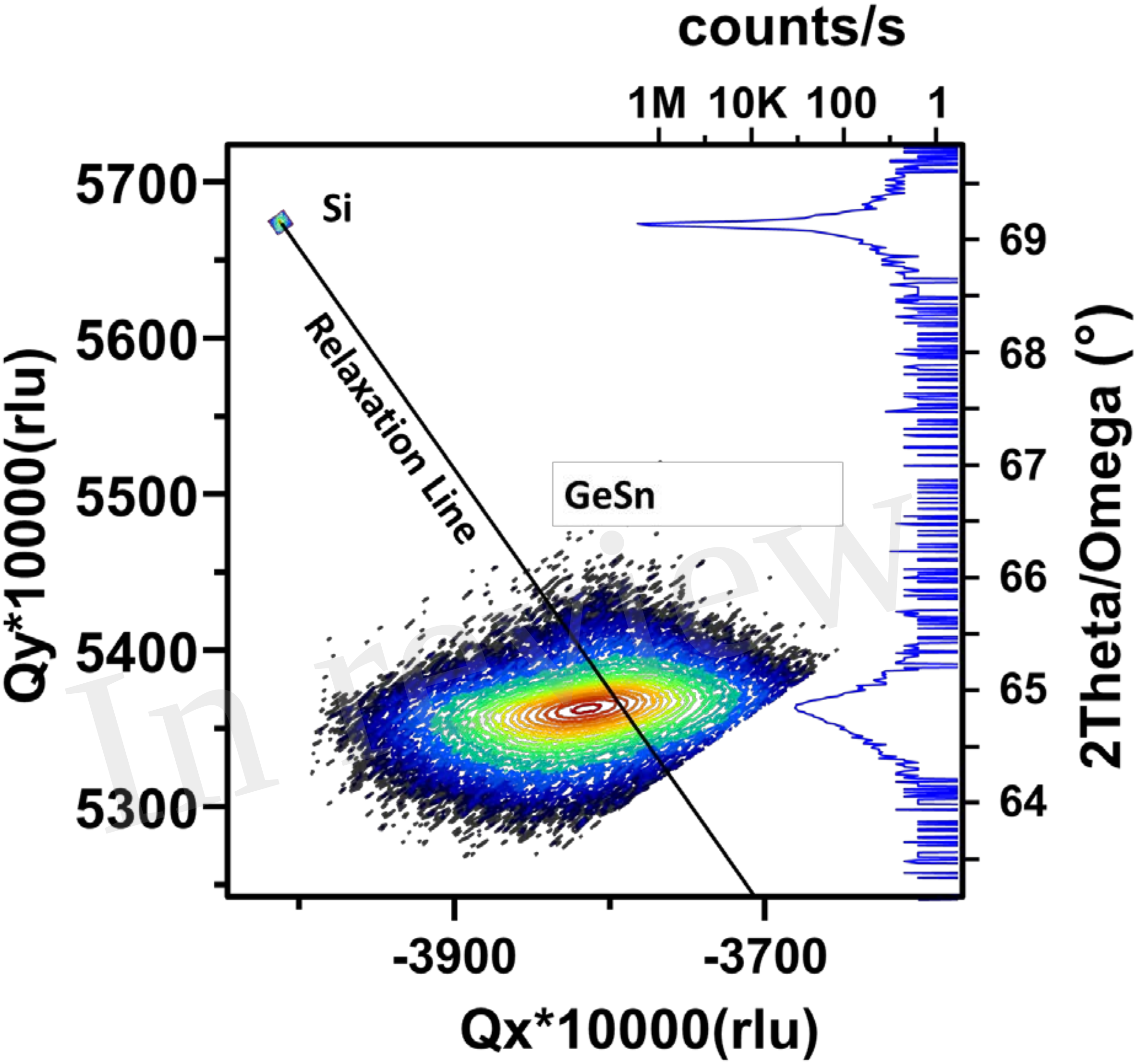
counts/s
1M
10K
100
1
5700
5600
5500
5400
5300
Qy*10000(rlu)
Si
Relaxation Line
GeSn
69
68
67
66
65
64
2Theta/Omega (°)
-3900
-3700
Qx*10000(rlu)

Figure 3

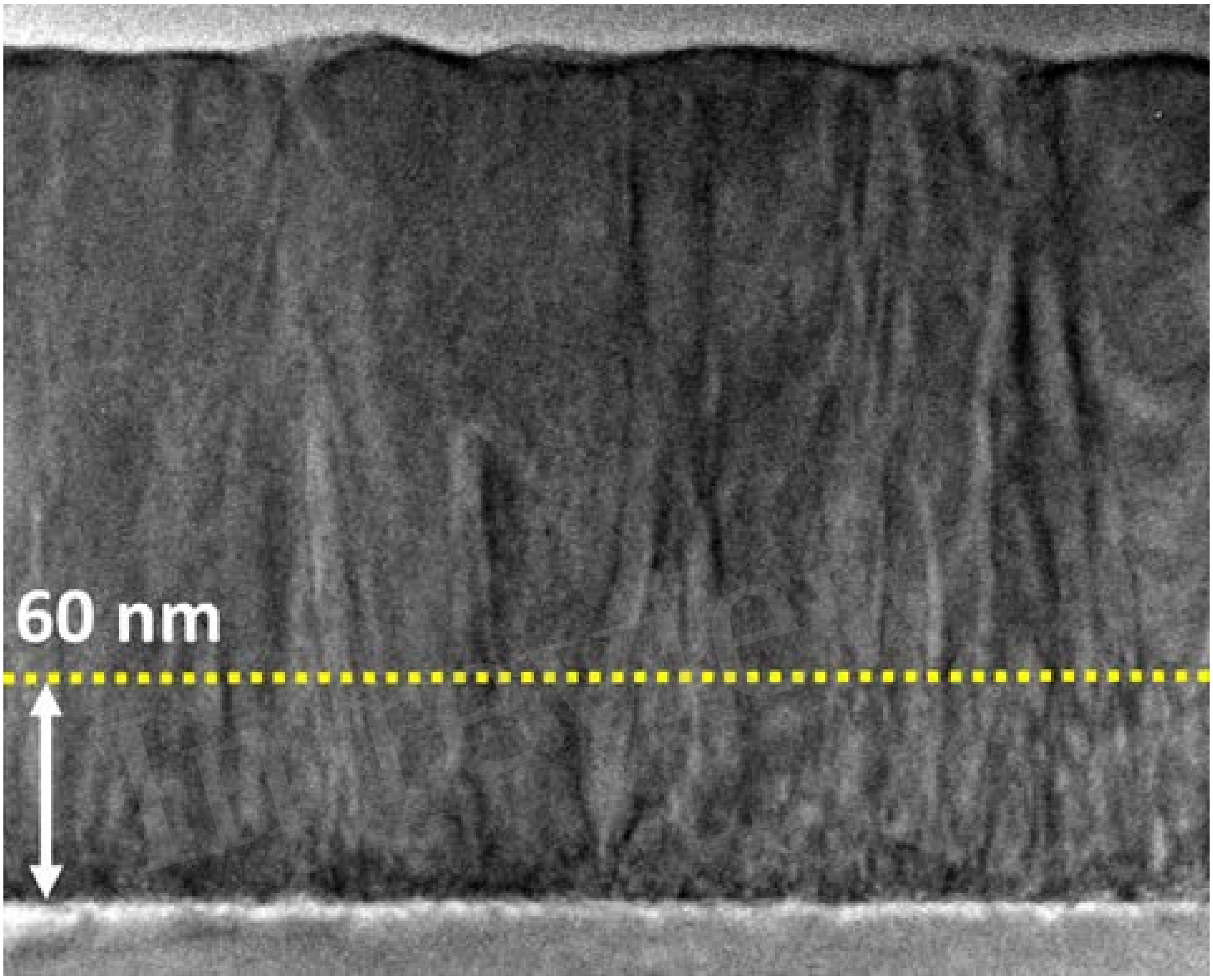

Figure 4

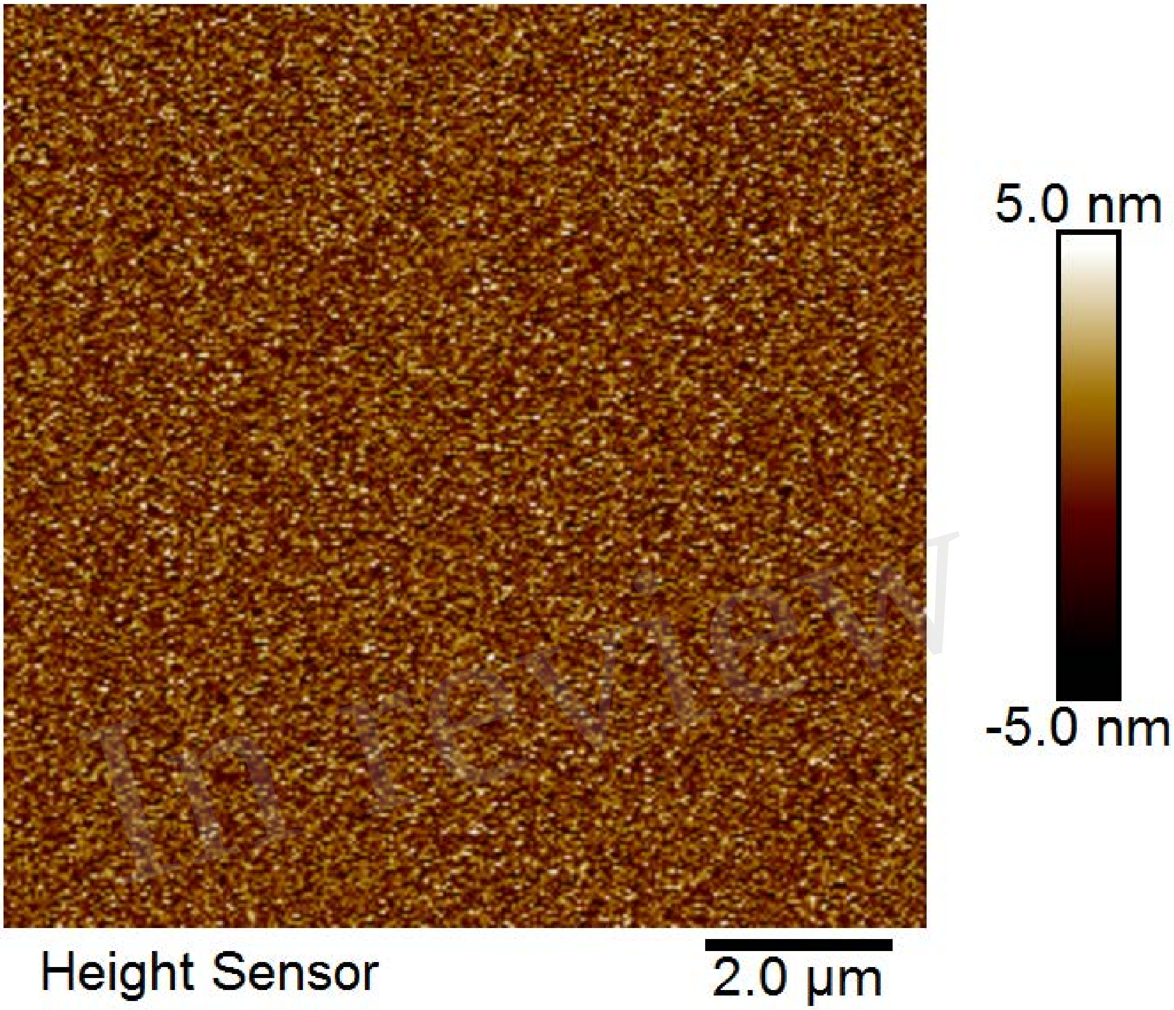

Figure 5

Figure 1.TIF

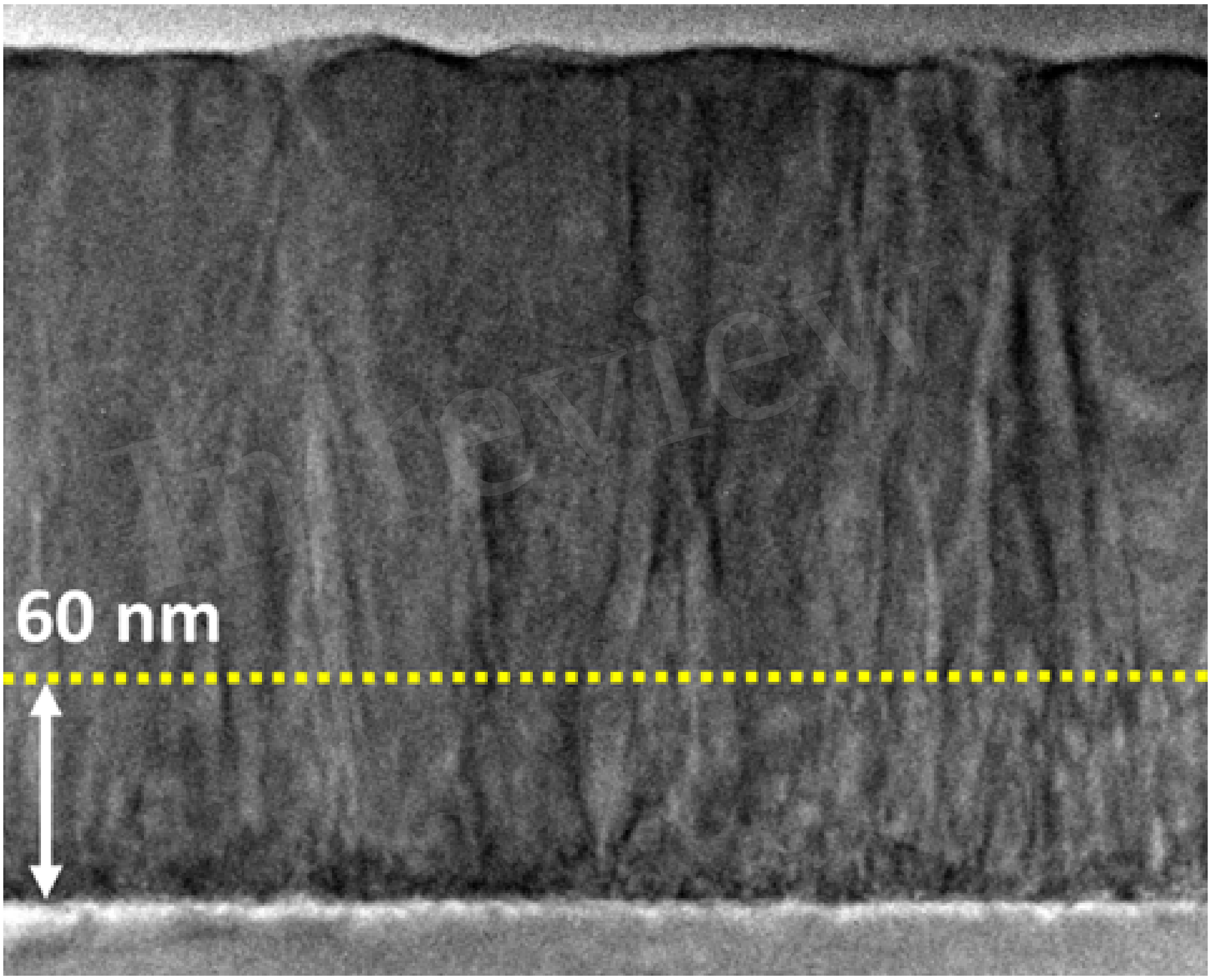

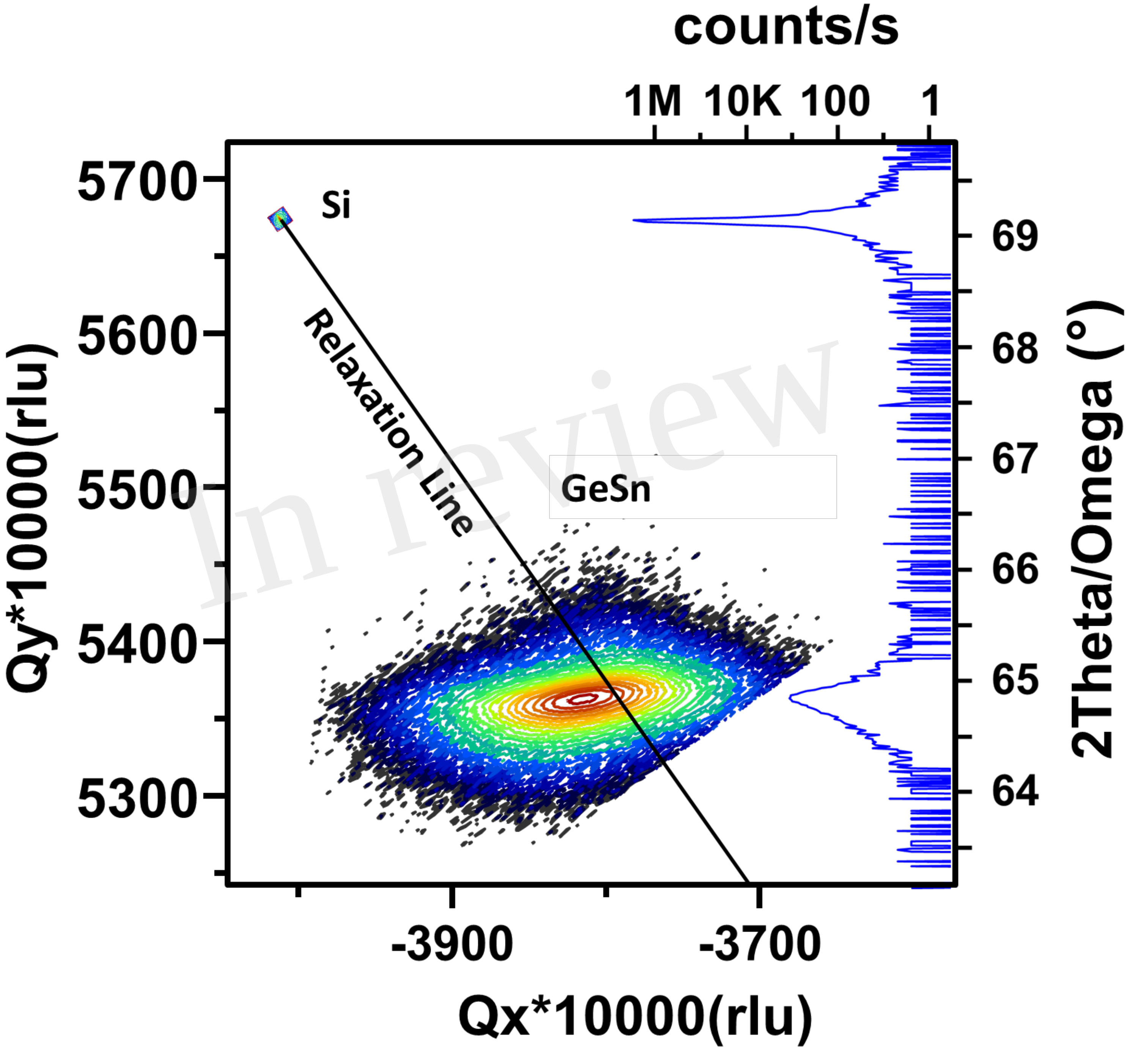
counts/s
1M
10K
100
1
5700
5600
5500
5400
5300
Qy*10000(rlu)
Si
Relaxation Line
GeSn
69
68
67
66
65
64
2Theta/Omega (°)
-3900
-3700
Qx*10000(rlu)

Figure 3.TIF

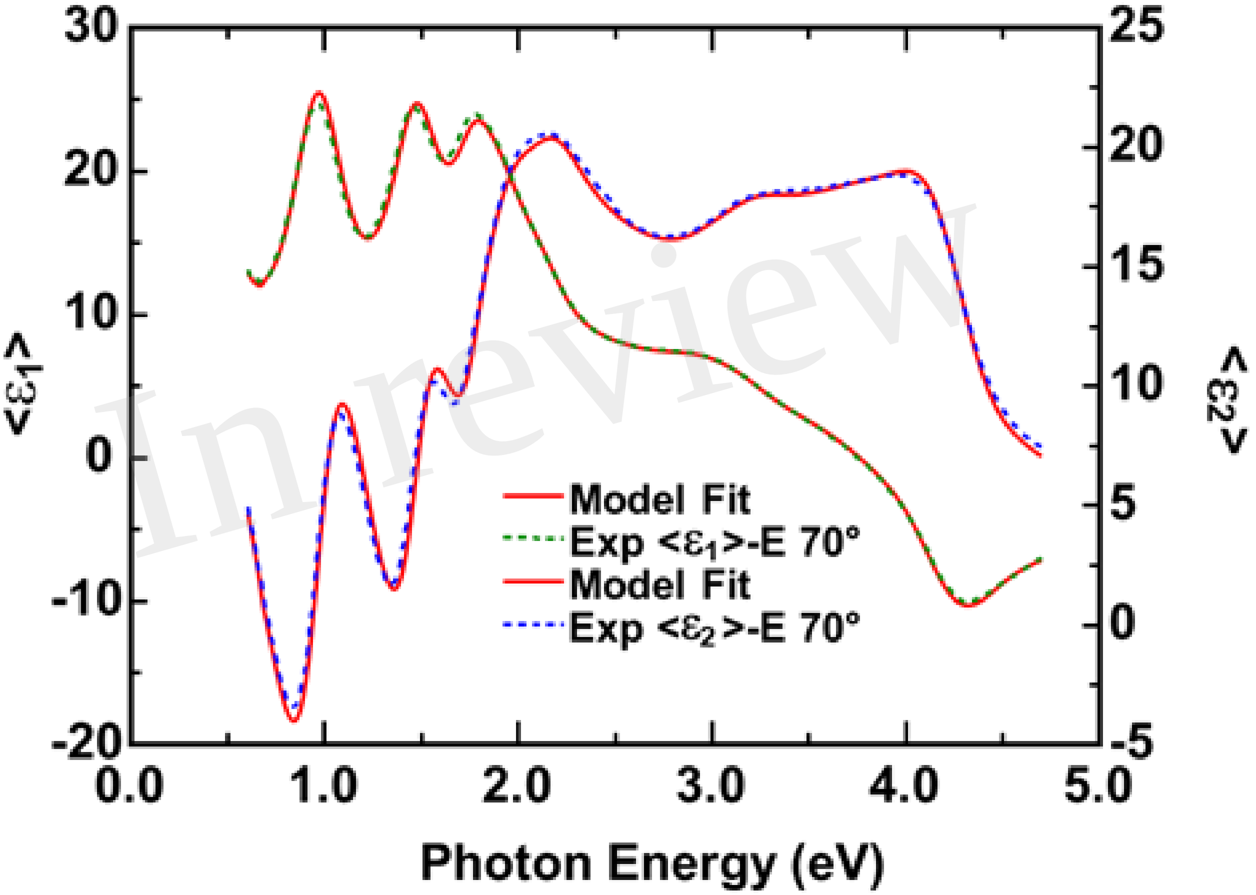
30
20
10
0
-10
-20
25
20
15
10
5
0
-5
0.0
1.0
2.0
3.0
4.0
5.0
Photon Energy (eV)
<ε1>
<ε2>
Model Fit
Exp <ε1>-E 70°
Model Fit
Exp <ε2>-E 70°

Figure 4.TIF

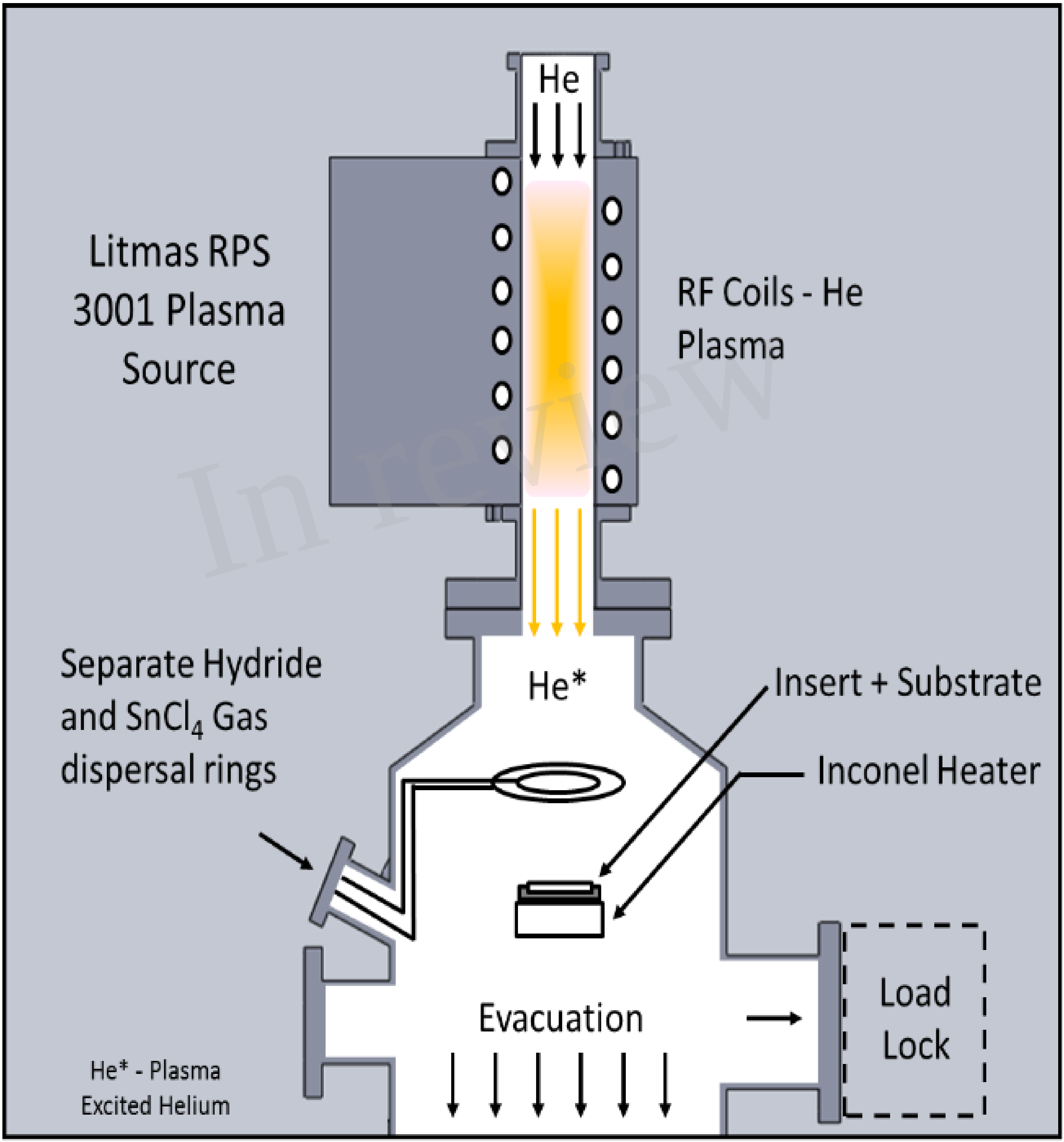
He
Litmas RPS 3001 Plasma Source
RF Coils - He Plasma
He*
Separate Hydride and $SnCl_4$ Gas dispersal rings
Insert + Substrate
Inconel Heater
Evacuation
Load Lock
He* - Plasma Excited Helium

Figure 5.TIF